High-temperature superfluidity of the two-component Bose gas in a transition metal dichalcogenide bilayer

Oleg L. Berman and Roman Ya. Kezerashvili

Physics Department, New York City College of Technology, The City University of New York, Brooklyn, New York 11201, USA and The Graduate School and University Center, The City University of New York, New York, New York 10016, USA

(Received 1 February 2016; revised manuscript received 27 April 2016; published 13 June 2016)

The high-temperature superfluidity of two-dimensional dipolar excitons in two parallel transition metal dichalcogenide (TMDC) layers is predicted. We study Bose-Einstein condensation in the two-component system of dipolar A and B excitons. The effective mass, energy spectrum of the collective excitations, the sound velocity, and critical temperature are obtained for different TMDC materials. It is shown that in the Bogoliubov approximation, the sound velocity in the two-component dilute exciton Bose gas is always larger than in any one-component exciton system. The difference between the sound velocities for two-component and one-component dilute gases is caused by the fact that the sound velocity for a two-component system depends on the reduced mass of A and B excitons, which is always smaller than the individual mass of A or B exciton. Due to this fact, the critical temperature T_c for superfluidity for the two-component exciton system in a TMDC bilayer is about one order of magnitude higher than T_c in any one-component exciton system. We propose to observe the superfluidity of two-dimensional dipolar excitons in two parallel TMDC layers, which causes two opposite superconducting currents in each TMDC layer.

DOI: 10.1103/PhysRevB.93.245410

I. INTRODUCTION

The phenomenon known as Bose-Einstein condensation (BEC) occurs when a substantial fraction of the bosons at low temperatures spontaneously occupy the single lowest-energy quantum state [1,2]. A BEC of bosons can exhibit superfluidity similar to superfluid helium [3,4]. A BEC of weakly interacting particles was achieved experimentally in gases of rubidium [5,6] and sodium [7,8] atoms. Cornell, Ketterle, and Wieman shared the 2001 Nobel Prize in Physics "for the achievement of BEC in dilute gases of alkali atoms." Enormous technical challenges had to be overcome in achieving the nanokelvin temperatures needed to create this atomic BEC. The experimental and theoretical achievements in the studies of the BEC of dilute supercold alkali gases are reviewed in Ref. [9].

The de Broglie wavelength of particles in a two-dimensional (2D) system is inversely proportional to the square root of the mass. Therefore, a BEC of small mass bosons can form at much higher temperatures than for relatively heavy alkali atoms. The very weakly bound boson quasiparticles can be produced using the absorption of a photon by a semiconductor causing the creation of an electron in a conduction band and a positively charge "hole" in a valence band. This electron-hole pair can form a bound state known as an "exciton." The mass of an exciton is much smaller than the mass of a regular atom. Therefore, such excitons are expected to undergo BEC and form a superfluid at experimentally observed exciton densities at temperatures much higher than for alkali atoms [10].

The prediction of superfluidity and BEC of dipolar (indirect) excitons formed by spatially separated electrons and holes in semiconductor coupled quantum wells (CQWs) attracted interest to this system [11–20]. In the CQWs, negative electrons are trapped in a two-dimensional plane, while an equal number of positive holes are located in a parallel plane at a distance D away. In this system, the electron-hole recombination due to the tunneling of electrons and holes between different quantum wells is suppressed by the dielectric barrier that separates the quantum wells. So, the excitons can have a very long lifetime [10] and, therefore, they can be treated as metastable particles described by quasiequilibrium statistics. At large enough separation distance D, the excitons experience the dipole-dipole repulsive interaction.

In the last decade, many experimental and theoretical studies were devoted to graphene, which is a 2D atomic plane of carbon atoms, known for unusual properties in its band structure [21,22]. The condensation of electron-hole pairs formed by spatially separated electrons and holes in two parallel graphene layers has been studied in Refs. [23–28]. The excitons in gapped graphene can be created by laser pumping. The superfluidity of quasi-two-dimensional dipolar excitons in two parallel graphene layers in the presence of band gaps was predicted recently in Ref. [29].

Today, an intriguing counterpart to gapless graphene is a class of monolayer direct band-gap materials, namely, transition metal dichalcogenides (TMDCs). Monolayers of TMDC such as MoS_2, $MoSe_2$, $MoTe_2$, WS_2, WSe_2, and WTe_2 are 2D semiconductors (below for TMDC monolayer we use the chemical formula MX_2, where M denotes a transition metal $M =$ Mo or W, and X denotes a chalcogenide $X =$ S, Se, or Te) which have a variety of applications in electronics and optoelectronics [30]. The strong interest in TMDC monolayers is motivated by the following properties: a semiconductor band structure characterized by a direct gap in the single-particle spectrum [31–34], the existence of excitonic valley physics [35,36], and the demonstration of electrically tunable, strong light-matter interactions [37,38]. The electronic band structure of TMDC monolayers was calculated [39] by applying the semiempirical tight-binding method [40] and the nonrelativistic augmented-plane-wave method [41]. The band structures and corresponding effective-mass parameters have been calculated for bulk, monolayer, and bilayer TMDCs in the GW approximation, by solving

the Bethe-Salpeter equation (BSE) [42–45] and using an analytical approach [46]. The properties of direct excitons in monolayer and few-layer TMDCs on a SiO_2 substrate were experimentally and theoretically investigated, identifying and characterizing not only the ground-state exciton but the full sequence of excited (Rydberg) exciton states [47]. The exciton binding energy for monolayer, few-layer, and bulk TMDCs and optical gaps were evaluated using the tight-binding approximation [48], by solving the BSE [49,50], applying an effective mass model, density functional theory and subsequent random phase approximation calculations [51], and by a generalized time-dependent density-matrix functional theory approach [52]. Significant spin-orbit splitting in the valence band leads to the formation of two distinct types of excitons in TMDC layers, labeled A and B [51]. Type A excitons are formed by spin-up electrons from conduction and spin-down holes from valence bands. Type B excitons are formed by spin-down electrons from conduction and spin-up holes from valence bands. According to Fig. 4 in Ref. [30], the spin-orbit splitting in the valence band is much larger than in the conduction band. In the valence bands of both MoX_2 and WX_2, the energy for spin-down electrons is larger than for spin-up electrons. This spin-orbit splitting causes the experimentally observed energy difference between the A and B excitons [30]. Two-photon spectroscopy of excitons in monolayer TMDCs was studied using the BSE [53].

It was recently proposed that a heterostructure design consisting of two TMDC monolayers separated by an h-BN insulating barrier could be used to observe high-temperature superfluidity in these materials [54]. The emission of neutral and charged excitons was controlled by the gate voltage, temperature, and the helicity and power of optical excitation. The formation of indirect excitons in a heterostructure of MoS_2 and $MoSe_2$ monolayers on a Si-SiO_2 substrate was observed [55]. The dynamics of direct and indirect excitons in WSe_2 bilayers was studied experimentally by applying time-resolved photoluminescence spectroscopy [56]. A phase transition that occurs between states containing one and two condensate components in two-dimensional spatially indirect exciton condensates in a TMDC bilayer was studied in Ref. [57]. We propose a theoretical description for the superfluidity of two-component Bose gas of such dipolar excitons in various TMDC bilayers.

The presence of a two-component mixture of A and B excitons in TMDC bilayers contributes significantly to the phenomenon of high-temperature superfluidity in these systems. Two-component mixtures of trapped cold atoms experiencing BEC and superfluidity have been the subject of various experimental and theoretical studies [58–61]. The Hamiltonian of two-component Bose systems includes three terms corresponding to each type of interaction in the system: two terms for the interaction of bosons of the same species, and one term for the interaction of bosons of different species. These three interaction terms in the Hamiltonian are described by three different interaction constants. The Bogoliubov approximation was previously developed and applied to describe the excitation spectrum of a two-component BEC of cold atoms [62–64]. We apply the Bogoliubov approximation here to derive the excitation spectrum of a two-component BEC of A and B dipolar excitons in a TMDC bilayer.

In this paper, we consider a dilute gas of dipolar excitons formed by an electron and a hole in two parallel, spatially separated TMDC monolayers. The spatial separation of electrons and holes in different monolayers results in an increase of the exciton lifetime compared to direct excitons in a single monolayer due to a relatively low probability of the tunneling between monolayers since the monolayers are separated by a dielectric barrier. We consider the formation of a BEC of A and B dipolar excitons that are in the ground state. To find the single-particle spectrum for a single dipolar exciton, we solve analytically the two-body problem for a spatially separated electron and hole located in two parallel TMDC layers. The latter step allows us to obtain the spectrum of the collective excitations and sound velocity for a dilute two-component exciton Bose gas formed by A and B excitons within the framework of the Bogoliubov approximation. The superfluid phase can be formed at finite temperatures due to the dipole-dipole interactions between dipolar excitons, which results in a soundlike spectrum at small momenta for the collective excitations. The sound spectrum satisfies the Landau criterion of superfluidity [65,66]. We calculated the spectrum of collective excitations, the density of a superfluid component as a function of temperature, and the mean field phase transition temperature, below which superfluidity occurs in this system. We predict the existence of high-temperature superfluidity of dipolar excitons in two TMDC layers at temperatures below the mean field phase transition temperature. Our most fascinating finding is that in the Bogoliubov approximation, the sound velocity in a two-component dilute Bose gas of indirect excitons is always larger than in any one-component Bose gas in CQWs, and that leads to remarkable high-temperature superfluidity.

The paper is organized in the following way. In Sec. II, we solve the eigenvalue problem for an electron and a hole in two different parallel TMDC layers, separated by a dielectric. The effective masses and single-particle energy spectra of dipolar excitons in two parallel TMDC layers are obtained. In Sec. III, we study the condensation of a two-component gas of dipolar A and B excitons and calculate the spectrum of collective excitations. In Sec. IV, we obtain the density of a superfluid component as well as the mean field phase transition temperature. The specific properties of the superfluid of direct excitons in a TMDC monolayer are discussed in Sec. V. The results of the calculations and their discussion are presented in Sec. VI. The conclusions follow in Sec. VII.

II. TWO-BODY PROBLEM FOR DIRAC PARTICLES WITH A GAP

The formation of excitons due to a gap opening in the electron-hole band structure in two parallel graphene layers separated by an insulator was studied in Ref. [29]. Here, we apply a similar approach to study excitons in coupled quantum wells designed from atomically thin materials stacked on top of each other and separated by a dielectric barrier. Let us consider indirect excitons composed of electrons and holes located in two different parallel TMDC monolayers separated by an insulating barrier of a thickness D as shown in Fig. 1. The choice for electrons and holes to be located at the top or bottom layer is arbitrary. The TMDC bilayer with spatially

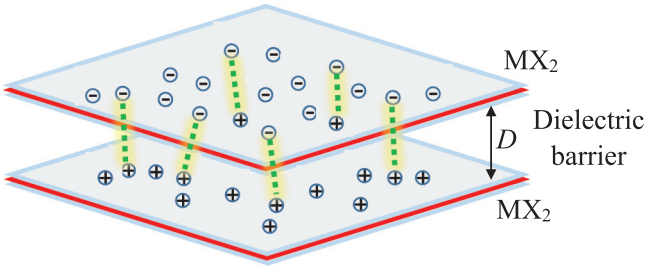

FIG. 1. Spatially separated electrons and holes in two TMDC monolayers.

separated electrons and holes can be designed by tuning the positions of the Fermi levels in individual layers, maintaining overall charge neutrality, either by applying a gate voltage between surrounding electrodes or a bias voltage between the TMDC layers [57]. Each monolayer TMDC has hexagonal lattice structure and consists of an atomic layer of a transition metal M sandwiched between two layers of a chalcogenide X in a trigonal prismatic structure as shown in Fig. 2.

In TMDC materials, the physics around the K and $-K$ points has attracted the most attention both experimentally and theoretically. Today, the gapped Dirac Hamiltonian model, which contains only the terms linear in p and the spin splitting in the valence band, is widely used [35]. The low-energy effective two-band single-electron Hamiltonian in the form of a spinor with a gapped spectrum for TMDCs in the $k \cdot p$ approximation is given by [35]

$$\hat{H}_s = at(\tau k_x \hat{\sigma}_x + k_y \hat{\sigma}_y) + \frac{\Delta}{2}\hat{\sigma}_z - \lambda\tau\frac{\hat{\sigma}_z - 1}{2}\hat{s}_z. \qquad (1)$$

In Eq. (1), $\hat{\sigma}$ denotes the Pauli matrices, a is the lattice constant, t is the effective hopping integral, Δ is the energy gap, $\tau = \pm 1$ is the valley index, 2λ is the spin splitting at the valence band top caused by the spin-orbit coupling (SOC), and $\hat{s}_z$ is the Pauli matrix for spin that remains a good quantum number. The parameters of the Hamiltonian $\hat{H}_s$ presented by Eq. (1) for transition metal dichalcogenides MoS_2, $MoSe_2$, WS_2, and WSe_2 are listed in Refs. [30,35], and in Ref. [30] the parameters for $MoTe_2$ and WTe_2 are presented.

We consider two parallel TMDC layers with an interlayer separation D. The dipolar excitons in this double-layer system are formed by the electrons located in one TMDC layer, while the holes are located in the parallel layer. Let us mention that the electron moves in one TMDC layer, and the hole moves in the other TMDC layer. So, the coordinate vectors of the

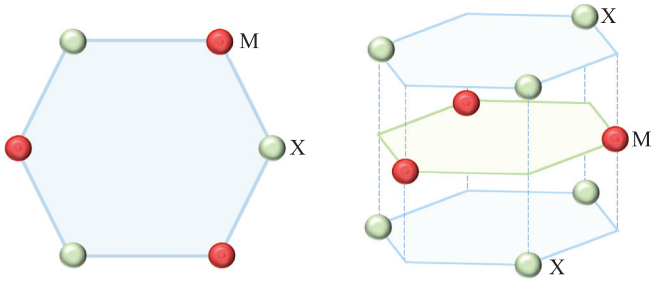

FIG. 2. The structure of a TMDC monolayer.

electron and hole can be replaced by their 2D projections onto the plane of one TMDC layer. These new in-plane coordinates $\mathbf{r}_1$ and $\mathbf{r}_2$ for an electron and a hole, correspondingly, will be used everywhere below. In each TMDC layer, a quasiparticle is characterized by the coordinates $\mathbf{r}_j$ in the conduction (c) and valence (v) band with the corresponding direction of spin (s_j) up $\uparrow$ or down $\downarrow$, and index $j = 1,2$ referring to the two monolayers, one with electrons and the other with holes. The spin basis for description of two particles in different monolayers is given by $\{|\Psi_{jc},s_{jc}\rangle,|\Psi_{jv},s_{jv}\rangle\}$, where $|\Psi_{jc},s_{jc}\rangle = |\Psi_{jc}\rangle \otimes |s_{jc}\rangle$ and $|\Psi_{jv},s_{jv}\rangle = |\Psi_{jv}\rangle \otimes |s_{jv}\rangle$ with the coordinate wave functions $|\Psi_{jc}\rangle$ and $|\Psi_{jv}\rangle$ and spin wave functions $|s_{jc}\rangle$ and $|s_{jv}\rangle$, where $s = \{\uparrow, \downarrow\}$ denotes the spin degree of freedom in the conduction and valence bands for the first and second monolayers, respectively. Therefore, the two-particle wave function that describes the bound electron and hole in different monolayers reads as $\Psi_s(\mathbf{r}_1,\mathbf{r}_2)$. This wave function can also be understood as a four-component spinor, where the spinor components refer to the four possible values of the conduction/valence band indices:

$$\Psi_\uparrow(\mathbf{r}_1,\mathbf{r}_2) = \begin{pmatrix} \phi_{c\uparrow c\uparrow}(\mathbf{r}_1,\mathbf{r}_2) \\ \phi_{c\uparrow v\uparrow}(\mathbf{r}_1,\mathbf{r}_2) \\ \phi_{v\uparrow c\uparrow}(\mathbf{r}_1,\mathbf{r}_2) \\ \phi_{v\uparrow v\uparrow}(\mathbf{r}_1,\mathbf{r}_2) \end{pmatrix} \equiv \begin{pmatrix} \Psi_{c\uparrow} \\ \Psi_{v\uparrow} \end{pmatrix},$$

$$\text{where } \Psi_{c\uparrow} = \begin{pmatrix} \phi_{c\uparrow c\uparrow} \\ \phi_{c\uparrow v\uparrow} \end{pmatrix}, \quad \Psi_{v\uparrow} = \begin{pmatrix} \phi_{v\uparrow c\uparrow} \\ \phi_{v\uparrow v\uparrow} \end{pmatrix}. \qquad (2)$$

The two components reflect one particle being in the conduction (valence) band and the other particle being in the valence (conduction) band, correspondingly. Let us mention that while Eq. (2) represents the spin-up particles, the spin-down particles are represented by the same expression replacing $\uparrow$ by $\downarrow$.

Each TMDC layer has an energy gap. Following the procedure applied for double-layer gapped graphene in Ref. [67], the Hamiltonian $H_{\uparrow(\downarrow)}$ for spin-up (spin-down) particles can be written as

$$\mathcal{H}_{\uparrow(\downarrow)} = \begin{pmatrix} V(r) & d_2 & d_1 & 0 \\ d_2^\dagger & -\Delta' + V(r) & 0 & d_1 \\ d_1^\dagger & 0 & \Delta' + V(r) & d_2 \\ 0 & d_1^\dagger & d_2^\dagger & V(r) \end{pmatrix}, \qquad (3)$$

where $V(r)$ is the potential energy of the attraction between an electron and a hole, the parameter Δ' is defined as $\Delta' = \Delta - \lambda$ for spin-up particles, and $\Delta' = \Delta + \lambda$ for spin-down particles. In Eq. (3), $d_1 = at(-i\partial_{x_1} - \partial_{y_1})$, $d_2 = at(-i\partial_{x_2} - \partial_{y_2})$ and the corresponding Hermitian conjugates are $d_1^\dagger = at(-i\partial_{x_1} + \partial_{y_1})$, $d_2^\dagger = at(-i\partial_{x_2} + \partial_{y_2})$, where $\partial_x = \partial/\partial x$ and $\partial_y = \partial/\partial y$, x_1, y_1 and x_2, y_2 are the coordinates of vectors $\mathbf{r}_1$ and $\mathbf{r}_2$, correspondingly.

The single-particle energy spectrum of an electron-hole pair can be found by solving the eigenvalue problem for the Hamiltonian given by Eq. (3):

$$\mathcal{H}_{\uparrow(\downarrow)}\Psi_{\uparrow(\downarrow)} = \epsilon_{\uparrow(\downarrow)}\Psi_{\uparrow(\downarrow)}, \qquad (4)$$

where $\Psi_{\uparrow(\downarrow)}$ are four-component eigenfunctions as given in Eq. (2), and $\epsilon_{\uparrow(\downarrow)}$ is the single-particle energy spectrum for an electron-hole pair with the up- and down-spin orientation, correspondingly. In this notation, we assume that a spin-up

(-down) hole describes the absence of a spin-down (-up) valence electron.

For the Hamiltonian (3), the center-of-mass motion cannot be separated from the relative motion due the chiral nature of Dirac electrons in TMDCs. A similar conclusion was made for the two-particle problem in graphene in Ref. [68] and gapped graphene in Ref. [67]. Since the electron-hole Coulomb interaction depends only on the relative coordinate, we introduce the new "center-of-mass" coordinates in the plane of a TMDC layer:

$$\mathbf{R} = \alpha \mathbf{r}_1 + \beta \mathbf{r}_2,$$
$$\mathbf{r} = \mathbf{r}_1 - \mathbf{r}_2, \tag{5}$$

where the coefficients α and β are supposed to be found below from the condition of the separation of the coordinates of the center-of-mass and relative motion in the Hamiltonian in the one-dimensional equation for the corresponding component of the wave function.

We make the following ansatz to obtain the solution of Eq. (4):

$$\Psi_{j\uparrow(\downarrow)}(\mathbf{R},\mathbf{r}) = e^{i\mathbf{K}\cdot\mathbf{R}}\psi_{j\uparrow(\downarrow)}(\mathbf{r}), \tag{6}$$

and follow the procedure described for the two-body problem in double-layer gapped graphene in Ref. [67]. The solution of a two-particle problem is demonstrated in Appendix A. Equation (A15) describes the bound electron-hole system, and can be written in the following form:

$$\left[-F_1(\epsilon_{\uparrow(\downarrow)})\nabla_{\mathbf{r}}^2 + V(r)\right]\phi_{c\uparrow\ (\downarrow)v\uparrow(\downarrow)} = F_0'(\epsilon_{\uparrow(\downarrow)})\phi_{c\uparrow(\downarrow)v\uparrow(\downarrow)}, \tag{7}$$

where

$$F_1(\epsilon_{\uparrow(\downarrow)}) = \frac{2a^2t^2}{\epsilon_{\uparrow(\downarrow)}}, \quad F_0'(\epsilon_{\uparrow(\downarrow)}) = \epsilon_{\uparrow(\downarrow)} + \Delta' - \frac{a^2t^2\mathcal{K}^2}{2\epsilon_{\uparrow(\downarrow)}}. \tag{8}$$

We consider a spatially separated electron-hole pair in two parallel TMDC layers at large distances $D \gg a_B$, where a_B is the 2D Bohr radius of a dipolar exciton. For TMDC materials the Bohr radius of the dipolar exciton is found to be in the range from 1.5 Å for $MoTe_2$ [43] up to 3.9 Å for MoS_2 [69].

It is obvious that the electron and hole are interacting via the Coulomb potential. However, in general, the electron-hole interaction is affected by screening effects [51]. However, the screening effects are negligible at long range for electron-hole distances larger than the screening length ρ_0, and at long range the electron-hole interaction is described by the Coulomb potential [51]. The screening length is defined as $\rho_0 = 2\pi\chi_{2D}$, where χ_{2D} is the 2D polarizability of the planar material [70]. Substituting χ_{2D} from Ref. [51], we conclude that for TMDC ρ_0 is estimated as 38 Å for WS_2, 41 Å for MoS_2, 45 Å for WSe_2, 52 Å for $MoSe_2$. The binding energy for the dipolar exciton was estimated for two MoS_2 layers separated by N h-BN insulating layers from $N = 1$ up to $N = 6$ [54]. These dipolar excitons were observed experimentally for $N = 2$ [71]. We assume that the indirect excitons in TMDCs can survive for a larger interlayer separation D than in semiconductor coupled quantum wells because the thickness of a TMDC layer is fixed, while the spatial fluctuations of the thickness of the semiconductor quantum well affect the structure of the dipolar exciton.

Since for TMDCs the characteristic values for the 2D exciton Bohr radius are found to be much less than the characteristic values of the screening length ρ_0, the Coulomb potential describes the electron-hole interaction for $D \gtrsim \rho_0$. Otherwise, for $D < \rho_0$, the electron-hole interaction is described by the Keldysh potential due to screening effects [72]. The two-body electron-hole system interacting via the Keldysh potential has no analytical solution and can only be solved numerically. We solve the two-body electron-hole problem analytically for large interlayer distances $D > \rho_0$. In this case, the screening effects accounted for by the Keldysh potential are negligible, and therefore the potential energy $V(r)$ is

$$V(r) = -\frac{ke^2}{\epsilon_d\sqrt{r^2 + D^2}}, \tag{9}$$

where $k = 9 \times 10^9\ N \times m^2/C^2$, ϵ_d is the dielectric constant of the dielectric, which separates two TMDC layers. Assuming $r \ll D$, we approximate $V(r)$ by the first two terms of the Taylor series, and substituting

$$V(r) = -V_0 + \gamma r^2, \tag{10}$$

where

$$V_0 = \frac{ke^2}{\epsilon_d D}, \quad \gamma = \frac{ke^2}{2\epsilon_d D^3}, \tag{11}$$

into Eq. (7), one obtains the equation that has the form of the Schrödinger equation for the 2D isotropic harmonic oscillator:

$$\left[-F_1(\epsilon_{\uparrow(\downarrow)})\nabla_{\mathbf{r}}^2 + \gamma r^2\right]\phi_{c\uparrow(\downarrow)v\uparrow(\downarrow)} = F_0(\epsilon_{\uparrow(\downarrow)})\phi_{c\uparrow(\downarrow)v\uparrow(\downarrow)}, \tag{12}$$

where

$$F_0(\epsilon_{\uparrow(\downarrow)}) = \epsilon_{\uparrow(\downarrow)} + \Delta' + V_0 - \frac{a^2t^2\mathcal{K}^2}{2\epsilon_{\uparrow(\downarrow)}}. \tag{13}$$

The solution of the Schrödinger equation for the harmonic oscillator is well known and is given by

$$\frac{F_0(\epsilon_{\uparrow(\downarrow)})}{F_1(\epsilon_{\uparrow(\downarrow)})} = 2N\sqrt{\frac{\gamma}{F_1(\epsilon_{\uparrow(\downarrow)})}}, \tag{14}$$

where $N = 2\tilde{N} + |L| + 1$, and $\tilde{N} = \min(\tilde{n},\tilde{n}')$, $L = \tilde{n} - \tilde{n}'$, $\tilde{n}, \tilde{n}' = 0,1,2,3,\ldots$ are the quantum numbers of the 2D harmonic oscillator. The corresponding 2D wave function at $\mathcal{K} = 0$ in terms of associated Laguerre polynomials can be written as

$$\phi_{c\uparrow(\downarrow)v\uparrow(\downarrow)\tilde{N}\ L,\mathcal{K}=0}(r) = \frac{\tilde{N}!}{a_B^{|L|+1}\sqrt{\tilde{n}!\tilde{n}'!}}\mathrm{sgn}(L)^L r^{|L|-1/2}e^{-r^2/(4a_B^2)} \times L_{\tilde{N}}^{|L|}\left[r^2/\left(2a_B^2\right)\right]\frac{e^{-iL\phi}}{(2\pi)^{1/2}}, \tag{15}$$

where ϕ is the polar angle, $L_k^p(x)$ are the associated Laguerre polynomials. and the Bohr radius of the dipolar exciton a_B is given by

$$a_B = (\sqrt{F_1(\epsilon)}/(2\sqrt{\gamma}))^{1/2} = \left(\frac{at}{\sqrt{2\gamma|\epsilon|}}\right)^{1/2}. \tag{16}$$

Substituting Eqs. (8) and (13) into Eq. (14), we obtain

$$2\epsilon_{\uparrow(\downarrow)}^2 + 2(\Delta' + V_0)\epsilon_{\uparrow(\downarrow)} - \frac{8atN\sqrt{\gamma\epsilon_{\uparrow(\downarrow)}}}{\sqrt{2}} - a^2t^2\mathcal{K}^2 = 0. \tag{17}$$

The solution of Eq. (17) for the single-exciton spectrum is shown in Appendix B. From Eq. (B7), for the single-exciton spectrum one obtains

$$\epsilon_{A(B)} = x_0^2 + \frac{\hbar^2\mathcal{K}^2}{2M_{A(B)}}, \tag{18}$$

where $M_{A(B)}$ is the dipolar exciton effective mass given by

$$M_{A(B)} = \frac{C_{A(B)}\hbar^2}{2a^2t^2x_0}, \tag{19}$$

where the parameter $C_{A(B)}$ is defined in Appendix B by Eq. (B6) as

$$C_{A(B)} = 3x_0^3 + (\Delta' + V_0)x_0. \tag{20}$$

In Eqs. (18)–(20), the parameter x_0 defined by Eq. (B4) has the different value for A and B excitons.

The dipolar exciton binding energy is given by

$$E_{b\,A(B)} = -\left(x_0^2 - \Delta'\right). \tag{21}$$

In Eqs. (20) and (21), we assume $\Delta' = \Delta - \lambda$ for A excitons and $\Delta' = \Delta + \lambda$ for B excitons.

III. COLLECTIVE EXCITATIONS FOR SPATIALLY SEPARATED ELECTRONS AND HOLES

Let us consider the dilute limit for gases of electrons and holes in parallel TMDC layers spatially separated by a dielectric, when $n_A a_{B\,A}^2 \ll 1$ and $n_B a_{B\,B}^2 \ll 1$, where $n_{A(B)}$ and $a_{B\,A(B)}$ are the concentrations and effective exciton Bohr radii for A (B) dipolar excitons, correspondingly. In experiments, the exciton density in a WSe_2 monolayer was obtained up to $n = 5 \times 10^{11}$ cm^{-2} [73]. In the dilute limit, the dipolar A and B excitons are formed by the electron-hole pairs with the electrons and holes spatially separated in two different TMDC layers.

The Hamiltonian $\hat{H}$ of the 2D A and B interacting dipolar excitons is given by

$$\hat{H} = \hat{H}_A + \hat{H}_B + \hat{H}_I, \tag{22}$$

where $\hat{H}_{A(B)}$ are the Hamiltonians of A (B) excitons given by

$$\hat{H}_{A(B)} = \sum_{\mathbf{k}} E_{A(B)}(k) a_{\mathbf{k}A(B)}^\dagger a_{\mathbf{k}A(B)} + \frac{g_{AA(BB)}}{2S} \times \sum_{\mathbf{klm}} a_{\mathbf{k}A(B)}^\dagger a_{\mathbf{l}A(B)}^\dagger a_{A(B)\mathbf{m}} a_{A(B)\mathbf{k+l-m}}, \tag{23}$$

and $\hat{H}_I$ is the Hamiltonian of the interaction between A and B excitons given by

$$\hat{H}_I = \frac{g_{AB}}{S} \sum_{\mathbf{klm}} a_{\mathbf{k}A}^\dagger a_{\mathbf{l}B}^\dagger a_{B\mathbf{m}} a_{A\mathbf{k+l-m}}, \tag{24}$$

where $a_{\mathbf{k}A(B)}^\dagger$ and $a_{\mathbf{k}A(B)}$ are Bose creation and annihilation operators for A (B) dipolar excitons with the wave vector $\mathbf{k}$, S is the area of the system, $E_{A(B)}(k) \equiv \epsilon_{A(B)} = \varepsilon_{(0)A(B)}(k) + \mathcal{A}_{A(B)}$ is the energy spectrum of noninteracting A (B) dipolar excitons, $\varepsilon_{(0)A(B)}(k) = \hbar^2k^2/(2M_{A(B)})$, $M_{A(B)}$ is an effective mass of noninteracting dipolar excitons, $\mathcal{A}_{A(B)}$ is the constant, which depends on A (B) dipolar exciton binding energy and the gap, formed by a spin-orbit coupling for the A (B) dipolar exciton, $g_{AA(BB)}$ and g_{AB} are the interaction constants for the interaction between two A dipolar excitons, two B dipolar excitons with the same conduction band electron spin orientation, and for the interaction between A and B dipolar excitons with the opposite conduction band electron spin orientation.

In our approach, we neglect exchange effects in the exciton-exciton interactions in a bilayer, while in Ref. [48] the exchange effects in exciton-exciton interaction were considered for a monolayer. It would be instructive to compare these limiting cases. The distinction between excitons and bosons is caused by exchange effects [10]. While the exchange interaction is very important for direct excitons in a TMDC monolayer studied in Ref. [48], the exchange interactions in a spatially separated electron-hole system in a bilayer are suppressed due to the low tunneling probability coming from the shielding of the dipole-dipole interaction by the insulating barrier. Hence, at large interlayer separations, the exchange phenomena, caused by the distinction between excitons and bosons, can be neglected for the electron-hole bilayers [74]. Two dipolar excitons in a dilute bilayer system interact according to the dipole-dipole potential $U(R) = ke^2D^2/(\epsilon_d R^3)$, where R is the distance between excitonic dipoles. The probability of tunneling through the barrier of the dipole-dipole interaction can be described by the transmission coefficient T [74]:

$$T \sim \exp\left[-\frac{1}{\hbar}\int_{r_0}^{R_0} \sqrt{2M_{A(B)}[U(R) - \mu]}\, dR\right],$$

where μ is the chemical potential of the system, r_0 is the 2D radius of exciton, R_0 is the classical turning point for the dipole-dipole interaction determined from by condition $U(R_0) = \mu$. Note that the chemical potential μ for our very dilute system of dipolar excitons, a type of 2D weakly nonideal Bose gas, is typically very small. Since at large interlayer separation D the transmission coefficient T is very small, the dilute system of dipolar excitons in a bilayer can be treated by the formalism applicable for a boson system. In addition, for direct excitons it was shown that, in spite of the difference between separate excitons and bosons, the exciton gas is effectively a Bose gas [75]. Bosons comprising this gas are mixtures of separate excitons, and the nonbosonic nature of excitons leads only to a renormalization of the interaction between them.

We consider the dilute system, when the average distance between excitons is much larger than the interlayer separation D, which corresponds to the densities $n \ll 1/(\pi D^2)$. Since we assume that $D \gtrsim \rho_0$, the screening effects are negligible, and the interaction between the particles is described by the Coulomb potential. For example, for $D = 50$ Å, the exciton densities should be $n < 1.3 \times 10^{12}$ cm^{-2}.

In a dilute system with large interlayer separation D, two dipolar excitons at a distance R repel due to the dipole-dipole interaction potential $U(R) = ke^2D^2/(\epsilon_d R^3)$. Following the

procedure presented in Ref. [19], the interaction parameters for the exciton-exciton interaction in very dilute systems could be obtained assuming the exciton-exciton dipole-dipole repulsion exists only at distances between excitons greater than distance from the exciton to the classical turning point. The distance between two excitons cannot be less than this distance, which is determined by the conditions reflecting the fact that the energy of two excitons cannot exceed double the chemical potential of the system μ:

$$2\mathcal{A}_A + U(R_{0AA}) = 2\mu, \quad 2\mathcal{A}_B + U(R_{0BB}) = 2\mu,$$
$$\mathcal{A}_A + \mathcal{A}_B + U(R_{0AB}) = 2\mu, \tag{25}$$

where R_{0AA}, R_{0BB}, and R_{0AB} are distances between two dipolar excitons at the classical turning point for two A excitons, two B excitons, and one A and one B exciton, correspondingly. Let us mention that in thermodynamic equilibrium, the chemical potentials of A and B dipolar excitons are equal.

From Eq. (25), the following expressions are obtained:

$$R_{0AA} = \left(\frac{ke^2D^2}{2\epsilon_d(\mu - \mathcal{A}_A)}\right)^{1/3}, \quad R_{0BB} = \left(\frac{ke^2D^2}{2\epsilon_d(\mu - \mathcal{A}_B)}\right)^{1/3},$$
$$R_{0AB} = \left(\frac{ke^2D^2}{\epsilon_d(2\mu - \mathcal{A}_A - \mathcal{A}_B)}\right)^{1/3}. \tag{26}$$

Following the procedure presented in Ref. [19], one can obtain the interaction constants for the exciton-exciton interaction

$$g_{AA} = \frac{2\pi ke^2D^2}{\epsilon_d R_{0AA}}, \quad g_{BB} = \frac{2\pi ke^2D^2}{\epsilon_d R_{0BB}},$$
$$g_{AB} = \frac{2\pi ke^2D^2}{\epsilon_d R_{0AB}}. \tag{27}$$

We expect that at zero temperature $T = 0$ almost all A and B excitons belong to the BEC of A and B excitons. Therefore, we assume the formation of a binary mixture of BECs. We consider this binary mixture within the Bogoliubov approximation [66]. The Bogoliubov approximation for a weakly interacting Bose gas allows one to diagonalize the many-particle Hamiltonian, replacing the product of four operators in the interaction term by the product of two operators. This is justified under the assumption that most of the particles belong to BEC, and only the interactions between the condensate and noncondensate particles are taken into account, while the interactions between noncondensate particles are neglected. The condensate operators are replaced by numbers [65], and the resulting Hamiltonian is quadratic with respect to the creation and annihilation operators. Using the Bogoliubov approximation [66], generalized for a two-component weakly interacting Bose gas [62], we obtain the chemical potential μ of the entire exciton system by minimizing $\hat{H}_0 - \mu\hat{N}$ with respect to the 2D concentration n, where $\hat{N}$ denotes the number operator

$$\hat{N} = \sum_{\mathbf{k}} a^\dagger_{\mathbf{k}A} a_{\mathbf{k}A} + \sum_{\mathbf{k}} a^\dagger_{\mathbf{k}B} a_{\mathbf{k}B}, \tag{28}$$

and H_0 is the Hamiltonian describing the particles in the condensate with zero momentum $\mathbf{k} = 0$. In the Bologoiubov approximation, we assume $N = N_0$, $a^\dagger_{\mathbf{k}=0,A\,(B)} = \sqrt{N_{0A\,(B)}}e^{-i\Theta_{A\,(B)}}$, and $a_{\mathbf{k}=0,A\,(B)} = \sqrt{N_{0A\,(B)}}e^{i\Theta_{A\,(B)}}$, where N is the total number of all excitons, and N_0 is the number of all excitons in the condensate, $N_{0A\,(B)}$ and $\Theta_{A\,(B)}$ are the number and phase for A (B) excitons in the condensate. From Eqs. (22), (23), and (24), we obtain

$$\hat{H}_0 - \mu\hat{N} = S\Big[(\mathcal{A}_A - \mu)n_A + (\mathcal{A}_B - \mu)n_B + \frac{g_{AA}n_A^2}{2} + \frac{g_{BB}n_B^2}{2} + g_{AB}n_An_B\Big], \tag{29}$$

where n_A and n_B are the 2D concentrations of A and B excitons, correspondingly. The minimization of $\hat{H}_0 - \mu\hat{N}$ with respect to the number of A excitons $N_A = Sn_A$ results in

$$\mu - \mathcal{A}_A = g_{AA}n_A + g_{AB}n_B. \tag{30}$$

The minimization of $\hat{H}_0 - \mu\hat{N}$ with respect to the number of B excitons $N_B = Sn_B$ results in

$$\mu - \mathcal{A}_B = g_{BB}n_B + g_{AB}n_A. \tag{31}$$

From Eqs. (30) and (31), we obtain

$$2\mu - \mathcal{A}_A - \mathcal{A}_B = g_{AA}n_A + g_{BB}n_B + g_{AB}n, \tag{32}$$

where $n = n_A + n_B$ is the total 2D concentration of excitons.

Combining Eqs. (26), (27), (30), (31), and (32), one obtains the following system of three cubic equations for the interaction constants g_{AA}, g_{BB}, g_{AB}:

$$g_{AA}^3 - 2\mathcal{B}n_Ag_{AA} - 2\mathcal{B}n_Bg_{AB} = 0,$$
$$g_{BB}^3 - 2\mathcal{B}n_Bg_{BB} - 2\mathcal{B}n_Ag_{AB} = 0,$$
$$g_{AB}^3 - \mathcal{B}ng_{AB} - \mathcal{B}(n_Ag_{AA} + n_Bg_{BB}) = 0, \tag{33}$$

where B is defined as

$$\mathcal{B} = \frac{(2\pi)^3(ke^2D^2)^2}{\epsilon_d^2}. \tag{34}$$

Taking the sum of the top two equations in (33), we can replace Eq. (33) by the following system of three cubic equations:

$$g_{AA}^3 - 2\mathcal{B}n_Ag_{AA} - 2\mathcal{B}n_Bg_{AB} = 0,$$
$$g_{BB}^3 - 2\mathcal{B}n_Bg_{BB} - 2\mathcal{B}n_Ag_{AB} = 0,$$
$$2g_{AB}^3 = g_{AA}^3 + g_{BB}^3. \tag{35}$$

The interaction constants g_{AA}, g_{BB}, g_{AB} can be obtained from the solution of the system of three cubic equations represented by Eq. (35).

If the interaction constants for the exciton-exciton interaction are negative, the spectrum of collective excitations at small momenta is imaginary which reflects the instability of the excitonic ground state [76,77]. The system of equations (35) has all real and positive roots only if $g_{AA} = g_{BB} = g_{AB} \equiv g$. Substituting this condition into Eq. (35), we obtain

$$g^3 - 2\mathcal{B}(n_A + n_B)g = 0. \tag{36}$$

Using $n = n_A + n_B$, we get from Eq. (36) the following expression for g:

$$g = \sqrt{2\mathcal{B}n}. \tag{37}$$

Substituting $\mathcal{B}$ from Eq. (34) into Eq. (37), we obtain g as

$$g = \frac{4\pi k e^2 D^2 \sqrt{\pi n}}{\epsilon_d}. \tag{38}$$

Using the following notation,

$$G_{AA} = g_{AA} n_A = g n_A, \quad G_{BB} = g_{BB} n_B = g n_B, \quad G_{AB} = g_{AB}\sqrt{n_A n_B} = g\sqrt{n_A n_B}, \quad \omega_A(k) = \sqrt{\varepsilon_{(0)A}^2(k) + 2G_{AA}\varepsilon_{(0)A}(k)},$$
$$\omega_B(k) = \sqrt{\varepsilon_{(0)B}^2(k) + 2G_{BB}\varepsilon_{(0)B}(k)}, \tag{39}$$

we obtain two modes of the spectrum of Bose collective excitations $\varepsilon_j(k)$ in the Bogoliubov approximation for two-component weakly interacting Bose gas [64]

$$\varepsilon_j(k) = \sqrt{\frac{\omega_A^2(k) + \omega_B^2(k) + (-1)^{j-1}\sqrt{\left[\omega_A^2(k) - \omega_B^2(k)\right]^2 + (4G_{AB})^2 \varepsilon_{(0)A}(k)\varepsilon_{(0)B}(k)}}{2}}, \tag{40}$$

where $j = 1, 2$. We can note that $G_{AB}^2 = G_{AA} G_{BB}$.

In the limit of small momenta $p = \hbar k$, when $\varepsilon_{(0)A}(k) \ll G_{AA}$ and $\varepsilon_{(0)B}(k) \ll G_{BB}$, we expand the spectrum of collective excitations $\varepsilon_j(k)$ up to first order with respect to the momentum p and get two sound modes of the collective excitations $\varepsilon_j(p) = c_j p$, where c_j is the sound velocity given by

$$c_j = \sqrt{\frac{G_{AA}}{2M_A} + \frac{G_{BB}}{2M_B} + (-1)^{j-1}\sqrt{\left(\frac{G_{AA}}{2M_A} - \frac{G_{BB}}{2M_B}\right)^2 + \frac{G_{AB}^2}{M_A M_B}}}. \tag{41}$$

In the limit of large momenta, when $\varepsilon_{(0)A}(k) \gg G_{AA}$ and $\varepsilon_{(0)B}(k) \gg G_{BB}$, we get two parabolic modes of collective excitations with the spectra $\varepsilon_1(k) = \varepsilon_{(0)A}(k)$ and $\varepsilon_2(k) = \varepsilon_{(0)B}(k)$, if $M_A < M_B$ and if $M_A > M_B$ with the spectra $\varepsilon_1(k) = \varepsilon_{(0)B}(k)$ and $\varepsilon_2(k) = \varepsilon_{(0)A}(k)$.

The Hamiltonian $\hat{H}_{\rm col}$ of the collective excitations, corresponding to two branches of the spectrum, in the Bogoliubov approximation for the entire two-component system is given by [64]

$$\hat{H}_{\rm col} = \sum_{\mathbf{k}\neq 0} \varepsilon_1(k) \alpha_{1\mathbf{k}}^\dagger \alpha_{1\mathbf{k}} + \sum_{\mathbf{k}\neq 0} \varepsilon_2(k) \alpha_{2\mathbf{k}}^\dagger \alpha_{2\mathbf{k}}, \tag{42}$$

where $\alpha_{j\mathbf{k}}^\dagger$ and $\alpha_{j\mathbf{k}}$ are the creation and annihilation Bose operators for the quasiparticles with the energy dispersion corresponding to the jth mode of the spectrum of the collective excitations.

If A and B excitons do not interact, we set $g_{AB} = 0$ and $G_{AB} = 0$, and in the limit of the small momenta we get for the sound velocity $c_1 = \sqrt{\frac{G_{AA}}{M_A}}$ and $c_2 = \sqrt{\frac{G_{BB}}{M_B}}$, which agrees with the sound velocity in the Bogoliubov approximation for a one-component system [66].

If for simplicity we consider the specific case when the densities of A and B excitons are the same $n_A = n_B = n/2$, we get from Eq. (39)

$$G_{AA} = G_{BB} = G_{AB} = gn/2, \quad \omega_A(k) = \sqrt{\varepsilon_{(0)A}^2(k) + gn\varepsilon_{(0)A}(k)}, \quad \omega_B(k) = \sqrt{\varepsilon_{(0)B}^2(k) + gn\varepsilon_{(0)B}(k)}. \tag{43}$$

From Eq. (40), we get the spectrum of collective excitations

$$\varepsilon_j(k) = \sqrt{\frac{\omega_A^2(k) + \omega_B^2(k) + (-1)^{j-1}\sqrt{\left[\omega_A^2(k) - \omega_B^2(k)\right]^2 + 4g^2 n^2 \varepsilon_{(0)A}(k)\varepsilon_{(0)B}(k)}}{2}}, \tag{44}$$

and the sound velocity at $n_A = n_B = n/2$ is obtained as

$$c_j = \sqrt{\frac{gn}{2}\left(\frac{1}{2M_A} + \frac{1}{2M_B} + (-1)^{j-1}\sqrt{\left(\frac{1}{2M_A} - \frac{1}{2M_B}\right)^2 + \frac{1}{M_A M_B}}\right)}. \tag{45}$$

It follows from Eq. (45) that there is only one nonzero sound velocity at $n_A = n_B = n/2$ given by

$$c = \sqrt{\frac{gn}{2}\left(\frac{1}{M_A} + \frac{1}{M_B}\right)}. \tag{46}$$

Interestingly enough, if for a one-component system the sound velocity is inversely proportional to the square root of the mass of the exciton, $M_A^{-1/2}$ or $M_B^{-1/2}$, then for a two-component system it is inversely proportional to the square root of the reduced mass of two excitons $\mu_{AB}^{-1/2}$,

where $\mu_{AB} = M_A M_B/(M_A + M_B)$. Since $M_A > \mu_{AB}$ and $M_B > \mu_{AB}$, it is always true that $M_A^{-1/2} < \mu_{AB}^{-1/2}$ or $M_B^{-1/2} < \mu_{AB}^{-1/2}$. Thus, within the Bogoliubov approximation the sound velocity in a two-component system is always larger than in a one-component system.

IV. SUPERFLUIDITY

Since at small momenta the energy spectrum of quasiparticles in the weakly interacting gas of dipolar excitons is soundlike, this system satisfies the Landau criterion for superfluidity [65,66] . The critical velocity for the superfluidity is given by $v_c = \min(c_1, c_2)$ because the quasiparticles are created at the velocities above the velocity of sound for the lowest mode of the quasiparticle dispersion.

The density of the superfluid component $\rho_s(T)$ is defined as $\rho_s(T) = \rho - \rho_n(T)$, where $\rho = M_A n_A + M_B n_B$ is the total 2D density of the system and $\rho_n(T)$ is the density of the normal component. We define the normal component density $\rho_n(T)$ by the standard procedure [4]. Suppose that the exciton system moves with a velocity $\mathbf{u}$, which means that the superfluid component moves with the velocity $\mathbf{u}$. At nonzero temperatures T, dissipating quasiparticles will appear in this system. Since their density is small at low temperatures, one can assume that the gas of quasiparticles is an ideal Bose gas. To calculate the superfluid component density, we define the total mass current for a two-component Bose gas of quasiparticles in the frame of the moving superfluid component, as

$$\mathbf{J} = \int \frac{d^2p}{(2\pi\hbar)^2}\mathbf{p}\{f[\varepsilon_1(p) - \mathbf{pu}] + f[\varepsilon_2(p) - \mathbf{pu}]\}, \tag{47}$$

where $f[\varepsilon_1(p)] = \{\exp[\varepsilon_1(p)/(k_B T)] - 1\}^{-1}$ and $f[\varepsilon_2(p)] = \{\exp[\varepsilon_2(p)/(k_B T)] - 1\}^{-1}$ are the Bose-Einstein distribution function for the quasiparticles with the dispersions $\varepsilon_1(p)$ and $\varepsilon_2(p)$, respectively, and k_B is the Boltzmann constant. Expanding the expression under the integral in terms of $\mathbf{pu}/(k_B T)$ and restricting ourselves to the first-order term, we obtain

$$\mathbf{J} = -\frac{\mathbf{u}}{2}\int \frac{d^2p}{(2\pi\hbar)^2} p^2\left(\frac{\partial f[\varepsilon_1(p)]}{\partial \varepsilon_1(p)} + \frac{\partial f[\varepsilon_2(p)]}{\partial \varepsilon_2(p)}\right). \tag{48}$$

The density ρ_n of the normal component is defined as [4]

$$\mathbf{J} = \rho_n \mathbf{u}. \tag{49}$$

Using Eqs. (48) and (49), we obtain the density of the normal component as

$$\rho_n(T) = -\frac{1}{2}\int \frac{d^2p}{(2\pi\hbar)^2} p^2\left(\frac{\partial f[\varepsilon_1(p)]}{\partial \varepsilon_1(p)} + \frac{\partial f[\varepsilon_2(p)]}{\partial \varepsilon_2(p)}\right). \tag{50}$$

At small temperatures $k_B T \ll M_{A(B)} c_j^2$, the small momenta, corresponding to the conditions $\varepsilon_{(0)A}(k) \ll G_{AA}$ and $\varepsilon_{(0)B}(k) \ll G_{BB}$, provide the main contribution to the integral in the right-hand side of Eq. (50), which corresponds to the quasiparticles with the sound spectrum $\varepsilon_j(k) = c_j k$ with the sound velocity given by Eq. (41), resulting in

$$\rho_n(T) = \frac{3\zeta(3)}{2\pi\hbar^2} k_B^3 T^3\left(\frac{1}{c_1^4} + \frac{1}{c_2^4}\right), \tag{51}$$

where $\zeta(z)$ is the Riemann zeta function [$\zeta(3) \simeq 1.202$].

For high temperatures $k_B T \gg M_{A(B)} c_j^2$, the large momenta $M_{A(B)} c_j^2 \ll \varepsilon_{0A(B)}(k) \ll k_B T$ provide the main contribution to the integral in the right-hand side of Eq. (50), which corresponds to quasiparticles with a parabolic spectrum. Using the result for these values of momenta for a one-component system [4], one gets for high temperatures

$$\rho_n(T) = \begin{cases} \frac{k_B T}{2\pi\hbar^2}\left(M_A^2 \ln\frac{k_B T}{M_A c_1^2} + M_B^2 \ln\frac{k_B T}{M_B c_2^2}\right), & \text{if } M_A < M_B \\ \frac{k_B T}{2\pi\hbar^2}\left(M_A^2 \ln\frac{k_B T}{M_A c_2^2} + M_B^2 \ln\frac{k_B T}{M_B c_1^2}\right), & \text{if } M_A > M_B. \end{cases} \tag{52}$$

Neglecting the interaction between the quasiparticles, the mean field critical temperature T_c of the phase transition related to the occurrence of superfluidity is given by the condition $\rho_s(T_c) = 0$ [4]:

$$\rho_n(T_c) = \rho = M_A n_A + M_B n_B. \tag{53}$$

At small temperatures $k_B T \ll M_{A(B)} c_j^2$, substituting Eq. (51) into (53), we get

$$T_c = \left[\frac{2\pi\hbar^2\rho}{3\zeta(3) k_B^3\left(\frac{1}{c_1^4} + \frac{1}{c_2^4}\right)}\right]^{1/3}. \tag{54}$$

If T_c obtained from Eq. (54) satisfies to the condition $k_B T_c \ll M_{A(B)} c_j^2$, it is the correct value of the mean field critical temperature. Otherwise, at high temperatures $k_B T \gg M_{A(B)} c_j^2$, we obtain the critical temperature T_c from the solution of the equation

$$\rho = \begin{cases} \frac{k_B T_c}{2\pi\hbar^2}\left(M_A^2 \ln\frac{k_B T_c}{M_A c_1^2} + M_B^2 \ln\frac{k_B T_c}{M_B c_2^2}\right), & \text{if } M_A < M_B \\ \frac{k_B T_c}{2\pi\hbar^2}\left(M_A^2 \ln\frac{k_B T_c}{M_A c_2^2} + M_B^2 \ln\frac{k_B T_c}{M_B c_1^2}\right), & \text{if } M_A > M_B. \end{cases} \tag{55}$$

At $n_A = n_B = n/2$, we get the density of the normal component as

$$\rho_n(T) = \begin{cases} \frac{3\zeta(3) k_B^3 T^3}{2\pi\hbar^2 c^4}, & \text{at low temperatures} \\ \frac{k_B T}{2\pi\hbar^2}\left(M_A^2 \ln\frac{k_B T}{M_A c^2} + M_B^2 \ln\frac{k_B T}{M_B c^2}\right), & \text{at high temperatures.} \end{cases} \tag{56}$$

At $n_A = n_B = n/2$, for the low-temperature case we get the mean field critical temperature as

$$T_c = \left[\frac{2\pi\hbar^2\rho c^4}{3\zeta(3) k_B^3}\right]^{1/3}. \tag{57}$$

At first glance, Eq. (57) is the same as for the one-component exciton gas. However, applying Eq. (46), one obtains

$$T_c = \left[\frac{\pi\hbar^2 g^2 n^3}{12\zeta(3)} Q\right]^{1/3}, \tag{58}$$

where the parameter Q is defined as

$$Q = \frac{M_A + M_B}{(\mu_{AB})^2}, \tag{59}$$

and μ_{AB} is the reduced mass for two-component system of A and B excitons. For a one-component dilute exciton gas $Q_A = 1/M_A$ or $Q_B = 1/M_B$, that is always less than the value of Q for a two-component Bose gas of A and B dipolar excitons. Therefore, T_c is always higher for a two-component dilute dipolar exciton gas than for a one-component dilute dipolar exciton gas.

If T_c obtained from Eq. (58) satisfies the condition $k_B T_c \ll M_{A(B)}c^2$, it is the correct value of the mean field critical temperature. Otherwise, at high temperatures $k_B T \gg M_{A(B)}c^2$, we obtain the critical temperature T_c from the solution of the equation

$$\rho = \frac{k_B T_c}{2\pi\hbar^2}\left(M_A^2 \ln\frac{k_B T_c}{M_A c^2} + M_B^2 \ln\frac{k_B T_c}{M_B c^2}\right), \tag{60}$$

where $\rho = (M_A + M_B)n/2$.

V. TWO-COMPONENT DIRECT EXCITON SUPERFLUIDITY IN A TMDC MONOLAYER

Let us consider the two-component weakly interacting Bose gas of direct A and B excitons in a TMDC monolayer. The direct excitons of type A are formed by spin-up electrons from the conduction band and spin-down holes from the valence band in a TMDC monolayer.

There are two differences between a two-component weakly interacting Bose gas of A and B excitons in a TMDC monolayer and two parallel TMDC layers with spatially separated charge carriers. The first difference is that the effective mass of direct excitons in a TMDC monolayer is different from the effective mass of indirect excitons in two parallel TMDC layers given by Eq. (19). The second difference is that the interaction constant for the contact exciton-exciton repulsion for direct excitons in a TMDC monolayer is different from the interaction constant for the dipole-dipole exciton-exciton repulsion for dipolar excitons in two parallel TMDC layers given by Eq. (38).

As discussed in Refs. [78,79] for a dilute exciton gas, the excitons can be treated as bosons with a repulsive contact interaction. For small values of the wave vector k, the exciton-exciton interaction constant, describing the pairwise exciton-exciton repulsion between A and A (B and B) direct excitons, can be approximated by a contact potential

$$g_{AA(BB)} = \frac{6ke^2 a_{A(B)}}{\varepsilon_m}, \tag{61}$$

where $a_{A(B)}$ is the exciton Bohr radius for A (B) direct excitons, correspondingly. This direct exciton Bohr radius $a_{A(B)}$ can be obtained analogously to $\tilde{\beta}$ in Eq. (39) in Ref. [67] for a gapped graphene monolayer. In Eq. (61), ε_m is the dielectric constant for the media surrounding the TMDC monolayer, and for a freely suspended TMDC material in vacuum we have $\varepsilon_m = 1$. This approximation for the exciton-exciton repulsion is applicable because resonantly excited excitons have very small wave vectors [80].

For the interaction constant, describing the pair contact repulsion between A and B excitons, we use

$$g_{AB} = \frac{6ke^2 a_{AB}}{\varepsilon_m}, \tag{62}$$

where a_{AB} is the phenomenological parameter. Assuming the value of a_{AB} is the average of a_A and a_B, we have

$$a_{AB} = \frac{a_A + a_B}{2}. \tag{63}$$

For direct excitons in a TMDC monolayer, substituting the direct exciton effective masses $M_{A(B)}$ and the direct excitons interaction parameters $g_{AA(BB)}$ and g_{AB} into Eqs. (40) and (41), we obtain the two branches of the spectrum of collective excitations and the sound velocities for direct excitons in a TMDC monolayer. Then, substituting the sound velocities into Eqs. (51) and (54), we obtain the density of the superfluid component as a function of temperature and the mean field temperature of the superfluid phase transition for a two-component weakly interacting Bose gas of direct excitons in a TMDC monolayer.

Note that the extension of our approach for direct excitons in a TMDC monolayer can be performed only under the applied approximations. Since the collective excitation spectrum in Eqs. (39) and (40) is calculated under the assumption of a dilute system, whereby the minimum separation between excitons is greater than the classical turning point distance, our approach for the direct excitons in a TMDC monolayer is approximate. Let us mention that in Ref. [81] the similar method was applied for a one-component system of exciton polaritons, formed by excitons in a gapped graphene monolayer, embedded in a semiconductor microcavity, and microcavity photons. The approach presented in this section can be easily applied to study the two-component superfluidity of A and B exciton polaritons in a TMDC monolayer embedded in a microcavity, which was studied in Ref. [82].

VI. RESULTS AND DISCUSSION

In this section, we present the results of our calculations. Since the dipolar excitons were experimentally observed in two TMDC layers separated by h-BN insulating layers [71], we consider the same dielectric in calculations using the dielectric constant $\varepsilon_d = 7.1$. In our calculations, we use the parameters a, t, Δ, and λ for transition metal dichalcogenides MoS_2, $MoSe_2$, WS_2, and WSe_2 that are listed in Table I in Ref. [35] and for $MoTe_2$ and WTe_2 from Ref. [30]. The results of calculations for the effective masses of A and B excitons for the layer separation $D = 5$ nm obtained from Eq. (19) are represented in Table I.

According to Table I, the B excitons are heavier than the A excitons for all TMDC. One advantage of our approach is that it illustrates the dependence of the effective exciton masses on spin-orbit coupling resulting in the formation of two types of excitons A and B in TMDC and their dependence on the parameters a, t, and Δ. In addition, the results of our

TABLE I. Effective masses of A and B excitons for different TMDC materials in units of the free electron mass at the interlayer separation $D = 5$ nm.

	Mass of exciton					
Exciton type	MoS_2	$MoSe_2$	$MoTe_2$	WS_2	WSe_2	WTe_2
A	0.499	0.555	0.790	0.319	0.345	0.277
B	0.545	0.625	0.976	0.403	0.457	0.501

calculations show that the exciton effective mass very slightly depends on the distance between two parallel TMDC layers D.

The interaction constant g as a function of the interlayer separation D and exciton concentration n is represented in Fig. 3. According to Fig. 3, the effective interaction constant g increases with the increase of the interlayer separation D and the increase of the exciton concentration n. The mean field critical temperature T_c for the excitonic superfluidity obtained from Eq. (58) is represented in Table II. The critical temperature T_c was calculated for different TMDC at the moderated concentration of excitons $n = 3 \times 10^{11}\,\mathrm{cm}^{-2}$. Let us mention that for our calculations we used an exciton concentration $n = 3 \times 10^{11}\,\mathrm{cm}^{-2}$ which is smaller than the maximal exciton concentration obtained in experiment [73]: $n_{\max} = 5 \times 10^{11}\,\mathrm{cm}^{-2}$. The exciton concentration $n = 3 \times 10^{11}\,\mathrm{cm}^{-2}$ corresponds to the degenerate exciton Bose gas in the phase diagram [54]. While, in general, in a TMDC monolayer the electron-hole interaction is described by Keldysh's potential [72], we performed our calculations for a TMDC bilayer at the interlayer separation from $D = 4$ nm up to $D = 5$ nm, when the screening effects are negligible, and the electron-hole interaction is described by the Coulomb potential. For our calculations, we used values of the interlayer separation D that are larger than experimental values [71] for the following reasons: (i) the larger D leads to the increase of the potential barrier for electron-hole tunneling between the layers, which results in the increase of the exciton lifetime; (ii) the larger D leads to the increase of the exciton dipole moment, which increases the exciton-exciton dipole-dipole repulsion and, therefore, increases the sound velocity and the superfluid density, which results in the increase of the mean field critical temperature of superfluidity, which can be seen in Table II.

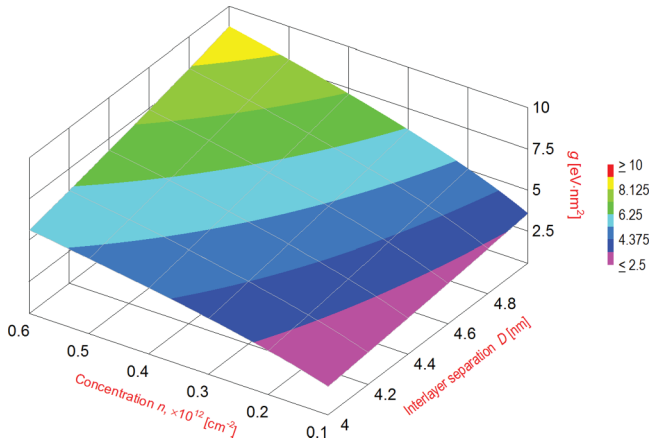

FIG. 3. Dependence of the interaction constant g on the exciton concentration n and interlayer separation D.

TABLE II. Dependence of the mean field critical temperature T_c on the interlayer separation D for different TMDC materials for the exciton concentration $n = 3 \times 10^{11}\,\mathrm{cm}^{-2}$.

D (nm)	T_c (K)					
	MoS_2	$MoSe_2$	$MoTe_2$	WS_2	WSe_2	WTe_2
4	55	53	47	63	61	64
5	74	71	63	85	82	87

The mean field critical temperature of superfluidity T_c as a function of the exciton concentration n for MX_2 materials is represented in Fig. 4. According to Fig. 4, the critical temperature T_c increases monotonically with the exciton concentration n, and T_c becomes progressively larger at a given concentration for different TMDCs in the following order: $MoTe_2$, $MoSe_2$, MoS_2, WSe_2, WS_2, WTe_2. The critical temperature T_c for all chalcogenides Se, S, and Te is larger for WX_2 than for MoX_2. It can be noticed that the order of types of different TMDC materials with respect to the increase of T_c, presented in Table II and Fig. 4, is exactly the same as the order of these TMDC materials with respect to the increase of the parameter Q, presented in Table III. This is caused by the fact that, according to Eq. (58), T_c is directly proportional to $Q^{1/3}$. Let us mention that the order of types of different TMDC materials with respect to the increase of T_c is different from the order of these materials with respect to the exciton effective masses, presented in Table I, and the parameters a, t, and the separation between X planes d_{X-X} taken from Ref. [30].

The exciton-exciton interaction studied in this paper for a two-component weakly interacting dilute system of A and B dipolar excitons leads to two branches of the collective excitation spectrum, characterized at small momenta by two different sound velocities c_1 and c_2, due to the fact that the system under consideration is a two-component system. Therefore, at small temperatures, the normal component is formed by the contributions from two types of quasiparticles, corresponding to two different branches of the collective excitations spectra with two different sound velocities at small momenta. All general expressions for the density of the normal and superfluid components and the mean field phase transition temperature were calculated in this paper, taking into account the existence of two branches of the spectrum of collective excitations. The calculations were presented for the specific case, when the concentrations of A and B excitons are equal, and the collective spectrum is characterized at small momenta by only one nonzero sound velocity.

We conclude that the critical temperature T_c for superfluidity for a two-component exciton gas in a TMDC bilayer is about one order of magnitude higher than T_c for one-component exciton gas in the semiconductor coupled quantum wells. According to Eq. (58), the mean field critical temperature T_c is directly proportional to the parameter $Q^{1/3}$, which is determined by the exciton reduced mass μ_{AB} and the sum of A and B exciton masses $M_A + M_B$, while for the one-component exciton Bose gas in CQWs $Q = M^{-1/3}$, where M is the exciton mass in CQWs. For example, if $M_A = M_B = M$, then Q for a one-component gas is eight times less than for a two-component Bose gas. Thus, for a one-component dilute exciton gas, Q is always less than the value of Q for a two-component Bose gas of A and B dipolar excitons. It can be

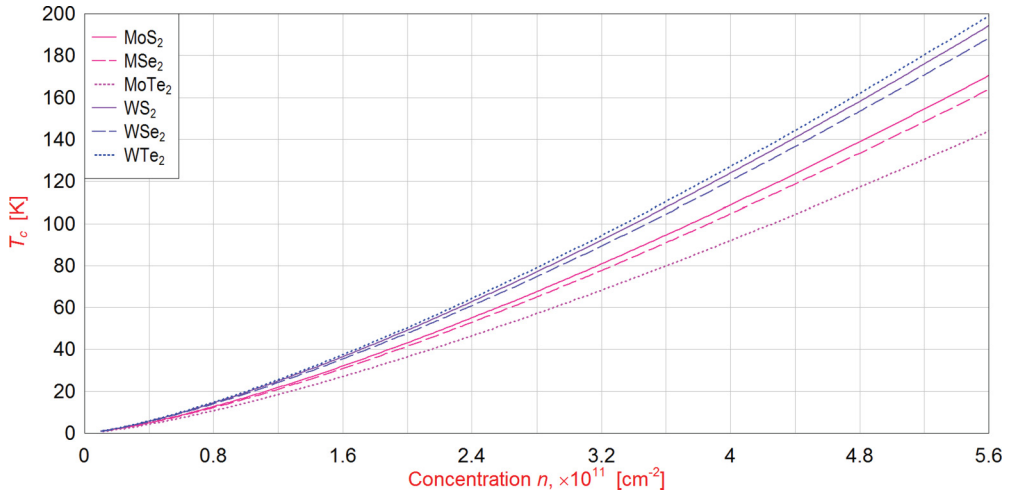

FIG. 4. The mean field critical temperature of the superfluidity T_c as a function of the exciton concentration n for different TMDC materials at the interlayer separation $D = 5$ nm.

easily seen that the inequalities $\mu_{AB} < M_A + M_B$ and $Q^{1/3} > (M_A + M_B)^{-1/3}$ are always true for any positive M_A and M_B. Therefore, T_c is always higher for a two-component dilute dipolar exciton gas than for any one-component dilute dipolar exciton gas in semiconductor CQWs in spite of the fact that the exciton masses for A and B excitons in CQWs are of the same order of magnitude as exciton masses in CQWs. Let us mention that in Ref. [57] the phase transition for indirect excitons in a TMDC bilayer from phase II, a phase with two condensate flavors, to phase I, a phase with only one condensate flavor, was studied. The authors found that a phase transition occurs between states containing one and two condensate components as the layer separation and the exciton density are varied. We study the superfluid-normal phase transition for the two-component system with A and B excitons, characterized by two different effective masses, when the effective mass difference is caused by the spin-orbit coupling. The mean field phase transition critical temperature T_c for a superfluid-normal phase transition for the two-component exciton gas in a TMDC bilayer is determined by the parameter Q, which is defined in Eq. (59). The advantage of the superfluidity of dipolar excitons in a TMDC bilayer lies in the possibility of creating a superconducting electric current in each TMDC layer by applying an external voltage, since electrons and holes in each monolayer are charge carriers. Thus, counterflow superfluidity can occur in a TMDC bilayer. Also, since the quasiparticle gap and the exciton binding energy in TMDC can be tuned by an externally applied voltage [83], the effective mass, the sound velocity for the collective excitations, the density of the superfluid component, and the phase transition temperature for superfluidity can also be controlled by an externally applied voltage.

TABLE III. Effective and reduced masses and factor Q for a two-component exciton gas of different TMDC materials at interlayer separation $D = 5$ nm.

	MoS_2	$MoSe_2$	$MoTe_2$	WS_2	WSe_2	WTe_2
$M_A + M_B$	1.044	1.180	1.766	0.722	0.802	0.778
μ_{AB}	0.261	0.294	0.437	0.178	0.197	0.179
Q	15.380	13.655	9.260	22.750	20.769	24.453

VII. CONCLUSIONS

We propose a physical realization to observe high-temperature superconducting electron-hole currents in two parallel TMDC layers, caused by the superfluidity of quasi-two-dimensional dipolar A and B excitons in a TMDC bilayer. The effective exciton masses for A and B excitons are calculated analytically. The spectrum of collective excitations obtained within the Bogoliubov approximation for TMDC bilayer is characterized by two branches, reflecting the fact that the exciton system under consideration is a two-component weakly interacting Bose gas of A and B excitons. Two sound velocities for both branches of the collective spectrum are derived for a two-component dipolar exciton system. It is shown that within the Bogoliubov approximation, the sound velocity in a two-component system is always larger than in a one-component system. The superfluid density, defined by the contributions from the collective excitations from two branches of collective spectrum, is obtained as a function of temperature for a two-component system of A and B dipolar excitons. We show that the superfluid density and the superfluid mean field phase transition temperature both increase with the increase of the excitonic concentration. The mean field critical temperature for the phase transition is analyzed for various TMDC materials. The mean field phase transition temperature, calculated for dipolar exciton bilayer, is about one order of magnitude higher than for any one-component exciton system of semiconductor CQWs due to the fact that T_c for a two-component exciton system in TMDCs depends on the exciton reduced mass for the two-component system of A and B excitons, more precisely, depends on the factor Q, which is much larger for a two-component system than for a one-component exciton system.

ACKNOWLEDGMENTS

The authors are grateful to A. Chernikov, M. Hybertsen, A. Moran, and D. Snoke for their valuable and stimulating discussions. This work is supported by the NSF Grant Supplement to the NSF Grant No. HRD-1345219.

APPENDIX A: EIGENVALUE PROBLEM FOR TWO PARTICLES

Let us introduce the following notations:

$$\mathcal{K}_+ = \mathcal{K}e^{i\Theta} = \mathcal{K}_x + i\mathcal{K}_y, \quad \mathcal{K}_- = \mathcal{K}e^{-i\Theta} = \mathcal{K}_x - i\mathcal{K}_y, \quad \Theta = \tan^{-1}\left(\frac{\mathcal{K}_y}{\mathcal{K}_x}\right), \tag{A1}$$

and represent the Hamiltonian (3) in the form of a 2×2 matrix as

$$\mathcal{H}_{\uparrow(\downarrow)} = \begin{pmatrix} \mathcal{O}_2 + V(r)\sigma_0 - \frac{\Delta'}{2}\sigma_0 + \frac{\Delta'}{2}\sigma_3 & \mathcal{O}_1 \\ \mathcal{O}_1^\dagger & \mathcal{O}_2 + V(r)\sigma_0 + \frac{\Delta'}{2}\sigma_0 + \frac{\Delta'}{2}\sigma_3 \end{pmatrix}, \tag{A2}$$

where $\mathcal{O}_1$ and $\mathcal{O}_2$ are given by

$$\mathcal{O}_1 = at(\,\alpha\mathcal{K}_- - i\,\partial_x - \partial_y)\sigma_0, \tag{A3}$$

$$\mathcal{O}_2 = -at\begin{pmatrix} 0 & \beta\mathcal{K}_- + i\,\partial_x + \partial_y \\ \beta\mathcal{K}_+ + i\,\partial_x - \partial_y & 0 \end{pmatrix}. \tag{A4}$$

In Eqs. (A3) and (A4), x and y are the components of vector $\mathbf{r}$, σ_j are the Pauli matrices, σ_0 is the 2×2 unit matrix.

The eigenvalue problem (4) for the Hamiltonian (A2) results in the following coupled equations:

$$\begin{aligned} &\left(\mathcal{O}_2 + V(r)\sigma_0 - \frac{\Delta'}{2}\sigma_0 + \frac{\Delta'}{2}\sigma_3\right)\Psi_{c\uparrow(\downarrow)} + \mathcal{O}_1\Psi_{v\uparrow(\downarrow)} = \epsilon_{\uparrow(\downarrow)}\sigma_0\Psi_{c\uparrow(\downarrow)}, \\ &\mathcal{O}_1^\dagger\Psi_{c\uparrow(\downarrow)} + \left(\mathcal{O}_2 + V(r)\sigma_0 + \frac{\Delta'}{2}\sigma_0 + \frac{\Delta'}{2}\sigma_3\right)\Psi_{v\uparrow(\downarrow)} = \epsilon_{\uparrow(\downarrow)}\sigma_0\Psi_{v\uparrow(\downarrow)}. \end{aligned} \tag{A5}$$

It follows from Eq. (A5) that

$$\Psi_{v\uparrow(\downarrow)} = \left(\epsilon_{\uparrow(\downarrow)}\sigma_0 - \mathcal{O}_2 - V(r)\sigma_0 - \frac{\Delta'}{2}\sigma_0 - \frac{\Delta'}{2}\sigma_3\right)^{-1}\mathcal{O}_1^\dagger\Psi_{c\uparrow(\downarrow)}. \tag{A6}$$

Assuming that the electron-hole attraction potential energy and both relative and center-of-mass kinetic energies are small compared to the gap Δ', the following approximation is applied:

$$\left(\epsilon_{\uparrow(\downarrow)}\sigma_0 - \mathcal{O}_2 - V(r)\sigma_0 - \frac{\Delta'}{2}\sigma_0 - \frac{\Delta'}{2}\sigma_3\right)^{-1} \simeq \left(\epsilon_{\uparrow(\downarrow)}\sigma_0 - \frac{\Delta'}{2}\sigma_0 - \frac{\Delta'}{2}\sigma_3\right)^{-1}. \tag{A7}$$

Applying

$$\mathcal{O}_1^\dagger\mathcal{O}_1 = a^2t^2\left[\alpha^2\mathcal{K}^2 - \nabla_{\mathbf{r}}^2 - 2i\alpha(\mathcal{K}_x\partial_y + \mathcal{K}_y\partial_x)\right]\sigma_0, \tag{A8}$$

and using Eq. (2) we obtain from Eq. (A5) for the individual spinor components the following equations:

$$\left[V(r) + \frac{a^2t^2\left[\alpha^2\mathcal{K}^2 - \nabla_{\mathbf{r}}^2 - 2i\alpha(\mathcal{K}_x\partial_x + \mathcal{K}_y\partial_y)\right]}{\epsilon_{\uparrow(\downarrow)} - \Delta'}\right]\phi_{c\uparrow(\downarrow)c\uparrow(\downarrow)} - at(\beta\mathcal{K}_- + i\,\partial_x + \partial_y)\phi_{c\uparrow(\downarrow)v\uparrow(\downarrow)} = \epsilon_{\uparrow(\downarrow)}\phi_{c\uparrow(\downarrow)c\uparrow(\downarrow)}, \tag{A9}$$

$$-at(\,\beta\mathcal{K}_+ + i\,\partial_x - \partial_y)\phi_{c\uparrow(\downarrow)c\uparrow(\downarrow)} + \left[V(r) - \Delta' + \frac{a^2t^2\left[\alpha^2\mathcal{K}^2 - \nabla_{\mathbf{r}}^2 - 2i\alpha(\mathcal{K}_x\partial_x + \mathcal{K}_y\partial_y)\right]}{\epsilon_{\uparrow(\downarrow)}}\right]\phi_{c\uparrow(\downarrow)v\uparrow(\downarrow)} = \epsilon_{\uparrow(\downarrow)}\phi_{c\uparrow(\downarrow)v\uparrow(\downarrow)}. \tag{A10}$$

Following the procedure applied for the calculation of the energy spectrum of the indirect excitons formed in two parallel gapped graphene layers [67], one gets from Eq. (A9) for the spinor component

$$\phi_{c\uparrow(\downarrow)c\uparrow(\downarrow)} = -\left(\epsilon_{\uparrow(\downarrow)} - V(r) - \frac{a^2t^2\left[\alpha^2\mathcal{K}^2 - \nabla_{\mathbf{r}}^2 - 2i\alpha(\mathcal{K}_x\partial_x + \mathcal{K}_y\partial_y)\right]}{\epsilon_{\uparrow(\downarrow)} - \Delta'}\right)^{-1}[at(\beta\mathcal{K}_- + i\,\partial_x + \partial_y)\phi_{c\uparrow(\downarrow)v\uparrow(\downarrow)}]. \tag{A11}$$

Assuming that the interaction potential and both the relative and center-of-mass kinetic energies are small compared to the exciton energy, we apply the following approximation:

$$\left[\epsilon_{\uparrow(\downarrow)} - V(r) - \frac{a^2t^2\left[\alpha^2\mathcal{K}^2 - \nabla_{\mathbf{r}}^2 - 2i\alpha(\mathcal{K}_x\partial_x + \mathcal{K}_y\partial_y)\right]}{\epsilon_{\uparrow(\downarrow)} - \Delta'}\right]^{-1} \approx \frac{1}{\epsilon_{\uparrow(\downarrow)}}. \tag{A12}$$

Substituting $\phi_{c\uparrow(\downarrow)c\uparrow(\downarrow)}$ from Eq. (A11) into (A10) and applying the approximation given by Eq. (A12), we obtain

$$\begin{aligned} &\left[-\Delta' + V(r) + \frac{a^2t^2\left[\beta^2\mathcal{K}^2 - \nabla_{\mathbf{r}}^2 + 2i\beta(\mathcal{K}_x\partial_x + \mathcal{K}_y\partial_y)\right]}{\epsilon_{\uparrow(\downarrow)}} + \frac{a^2t^2\left[\alpha^2\mathcal{K}^2 - \nabla_{\mathbf{r}}^2 - 2i\alpha(\mathcal{K}_x\partial_x + \mathcal{K}_y\partial_y)\right]}{\epsilon_{\uparrow(\downarrow)}}\right]\phi_{c\uparrow(\downarrow)v\uparrow(\downarrow)} \\ &\quad = \epsilon_{\uparrow(\downarrow)}\phi_{c\uparrow(\downarrow)v\uparrow(\downarrow)}. \end{aligned} \tag{A13}$$

Choosing the values of the coefficients α and β which will separate the coordinates of the center of mass (the wave vector $\mathcal{K}$) and relative motion $\mathbf{r}$ in Eq. (A13), we have

$$\alpha = \tfrac{1}{2}, \quad \beta = \tfrac{1}{2}. \tag{A14}$$

Substituting Eq. (A14) into (A13), we get

$$\left[-\frac{2a^2t^2\nabla_{\mathbf{r}}^2}{\epsilon_{\uparrow(\downarrow)}} + \frac{a^2t^2\mathcal{K}^2}{2\epsilon} - \Delta' + V(r)\right]\phi_{c\uparrow(\downarrow)v\uparrow(\downarrow)} = \epsilon_{\uparrow(\downarrow)}\phi_{c\uparrow(\downarrow)v\uparrow(\downarrow)}. \tag{A15}$$

APPENDIX B: SOLUTION OF THE EQUATION FOR THE SINGLE-EXCITON SPECTRUM

Introducing $x = \sqrt{\epsilon_{\uparrow(\downarrow)}}$, one rewrites Eq. (17) in the following form:

$$2x^4 + 2(\Delta' + V_0)x^2 - \frac{8atN\sqrt{\gamma}x}{\sqrt{2}} - a^2t^2\mathcal{K}^2 = 0. \tag{B1}$$

For small momenta $\hbar\mathcal{K}$, we assume

$$x = x_0 + \Delta x, \tag{B2}$$

where $x = x_0$ corresponds to $\mathcal{K} = 0$. In this case, we obtain from Eq. (B1) the following equation:

$$x_0^3 + (\Delta' + V_0)x_0 - \frac{4atN\sqrt{\gamma}}{\sqrt{2}} = 0. \tag{B3}$$

The cubic equation (B3) has the following real root:

$$x_0 = \left(\frac{q}{2} + \sqrt{\frac{q^2}{4} + \frac{p^3}{27}}\right)^{1/3} + \left(\frac{q}{2} - \sqrt{\frac{q^2}{4} + \frac{p^3}{27}}\right)^{1/3}, \tag{B4}$$

where the parameters p and q are given by

$$p = \Delta' + V_0, \quad q = \frac{4atN\sqrt{\gamma}}{\sqrt{2}}. \tag{B5}$$

Substituting Eq. (B2) into (B1), in the first order with respect to Δx, we obtain

$$\Delta x = \frac{a^2t^2\mathcal{K}^2}{2C_{A(B)}}, \quad C_{A(B)} = 3x_0^3 + (\Delta' + V_0)x_0, \tag{B6}$$

where C_A and C_B are related to the A and B excitons, when $\Delta' = \Delta - \lambda$ and $\Delta' = \Delta + \lambda$ are used for spin-down and spin-up particles, respectively. Let us also mention that the values of x_0 and Δx are different for different TMDC materials due to the different values of parameters a,t, Δ, and λ. Then, we get for the exciton energy ϵ for A (B) excitons to first order with respect to Δx:

$$\epsilon_{A\,(B)} = \epsilon_{\uparrow(\downarrow)} = (x_0 + \Delta x)^2 \approx x_0^2 + 2x_0\Delta x, \tag{B7}$$

where x_0 has the different values for A and B excitons.

[1] S. N. Bose, Z. Phys. **26**, 178 (1924).
[2] A. Einstein, Sitzungsberich. Preussisch. Akad. Wissenschaft. **1**, 3 (1925).
[3] A. Griffin, *Excitations in a Bose-condensed Liquid* (Cambridge University Press, Cambridge, UK, 1993).
[4] L. Pitaevskii and S. Stringari, *Bose-Einstein Condensation* (Clarendon, Oxford, 2003).
[5] M. H. Anderson and J. R. Ensher, Science **269**, 198 (1995).
[6] J. R. Ensher, D. S. Jin, M. R. Matthews, C. E. Wieman, and E. A. Cornell, Phys. Rev. Lett. **77**, 4984 (1996).
[7] W. Ketterle and N. J. van Druten, Phys. Rev. A **54**, 656 (1996).
[8] W. Ketterle and H.-J. Miesner, Phys. Rev. A **56**, 3291 (1997).
[9] F. Daflovo, S. Giorgini, and L. P. Pitaevskii, Rev. Mod. Phys. **71**, 463 (1999).
[10] S. A. Moskalenko and D. W. Snoke, *Bose-Einstein Condensation of Excitons and Biexcitons and Coherent Nonlinear Optics with Excitons* (Cambridge University Press, New York, 2000).
[11] Yu. E. Lozovik and V. I. Yudson, Zh. Eksp. Teor. Fiz. **71**, 738 (1976) [Sov. Phys. JETP **44**, 389 (1976)].
[12] X. Zhu, P. B. Littlewood, M. S. Hybertsen, and T. M. Rice, Phys. Rev. Lett. **74**, 1633 (1995).
[13] G. Vignale and A. H. MacDonald, Phys. Rev. Lett. **76**, 2786 (1996).
[14] M. A. Olivares-Robles and S. E. Ulloa, Phys. Rev. B **64**, 115302 (2001).
[15] D. W. Snoke, Science **298**, 1368 (2002).
[16] L. V. Butov, J. Phys.: Condens. Matter **16**, R1577 (2004).
[17] J. P. Eisenstein and A. H. MacDonald, Nature (London) **432**, 691 (2004).
[18] O. L. Berman, Yu. E. Lozovik, D. W. Snoke, and R. D. Coalson, Phys. Rev. B **70**, 235310 (2004).
[19] O. L. Berman, R. Ya. Kezerashvili, G. V. Kolmakov, and Yu. E. Lozovik, Phys. Rev. B **86**, 045108 (2012).
[20] Y. Ben-Aryeh, J. Supercond. Nov. Magn. **28**, 3211 (2015).
[21] A. H. Castro Neto, F. Guinea, N. M. R. Peres, K. S. Novoselov, and A. K. Geim, Rev. Mod. Phys. **81**, 109 (2009)
[22] S. Das Sarma, S. Adam, E. H. Hwang, and E. Rossi, Rev. Mod. Phys. **83**, 407 (2011).
[23] Yu. E. Lozovik and A. A. Sokolik, JETP Lett. **87**, 55 (2008).
[24] C.-H. Zhang and Y. N. Joglekar, Phys. Rev. B **77**, 233405 (2008).
[25] H. Min, R. Bistritzer, J.-J. Su, and A. H. MacDonald, Phys. Rev. B **78**, 121401(R) (2008).
[26] R. Bistritzer and A. H. MacDonald, Phys. Rev. Lett. **101**, 256406 (2008).
[27] M. Yu. Kharitonov and K. B. Efetov, Phys. Rev. B **78**, 241401(R) (2008).
[28] M. Zarenia, A. Perali, D. Neilson, and F. M. Peeters, Sci. Rep. **4**, 7319 (2014).
[29] O. L. Berman, R. Ya. Kezerashvili, and K. Ziegler, Phys. Rev. B **85**, 035418 (2012).
[30] A. Kormányos, G. Burkard, M. Gmitra, J. Fabian, V. Zólyomi, N. D. Drummond, and V. Fal'ko, 2D Mater. **2**, 022001 (2015).

[31] K. F. Mak, C. Lee, J. Hone, J. Shan, and T. F. Heinz, Phys. Rev. Lett. **105**, 136805 (2010).

[32] K. F. Mak, K. He, J. Shan, and T. F. Heinz, Nat. Nanotechnol. **7**, 494 (2012).

[33] L. Britnell, R. M. Ribeiro, A. Eckmann, R. Jalil, B. D. Belle, A. Mishchenko, Y.-J. Kim, R. V. Gorbachev, T. Georgiou, S. V. Morozov, A. N. Grigorenko, A. K. Geim, C. Casiraghi, A. H. Castro Neto, and K. S. Novoselov, Science **340**, 1311 (2013).

[34] W. Zhao, Z. Ghorannevis, L. Chu, M. Toh, C. Kloc, P.-H. Tan, and G. Eda, ACS Nano **7**, 791 (2013).

[35] D. Xiao, G.-B. Liu, W. Feng, X. Xu, and W. Yao, Phys. Rev. Lett. **108**, 196802 (2012).

[36] T. Cao *et al.*, Nat. Commun. **3**, 887 (2012).

[37] J. S. Ross, S. Wu, H. Yu, N. J. Ghimire, A. M. Jones, G. Aivazian, J. Yan, D. G. Mandrus, D. Xiao, W. Yao, and X. Xu, Nat. Commun. **4**, 1474 (2013).

[38] K. F. Mak *et al.*, Nat. Mater. **12**, 207 (2013).

[39] R. A. Bromley, R. B. Murray, and A. D. Yoffe, J. Phys. C: Solid State Phys. **5**, 759 (1972).

[40] R. A. Bromley and R. B. Murray, J. Phys. C: Solid State Phys. **5**, 738 (1972).

[41] L. F. Mattheis, Phys. Rev. B **8**, 3719 (1973).

[42] T. Cheiwchanchamnangij and W. R. L. Lambrecht, Phys. Rev. B **85**, 205302 (2012).

[43] A. Ramasubramaniam, Phys. Rev. B **86**, 115409 (2012).

[44] A. Molina-Sánchez, D. Sangalli, K. Hummer, A. Marini, and L. Wirtz, Phys. Rev. B **88**, 045412 (2013).

[45] F. Hüser, T. Olsen, and K. S. Thygesen, Phys. Rev. B **88**, 245309 (2013).

[46] G. Berghäuser and E. Malic, Phys. Rev. B **89**, 125309 (2014).

[47] A. Chernikov, T. C. Berkelbach, H. M. Hill, A. Rigosi, Y. Li, O. B. Aslan, D. R. Reichman, M. S. Hybertsen, and T. F. Heinz, Phys. Rev. Lett. **113**, 076802 (2014).

[48] F. Wu, F. Qu, and A. H. MacDonald, Phys. Rev. B **91**, 075310 (2015).

[49] H.-P. Komsa and A. V. Krasheninnikov, Phys. Rev. B **86**, 241201(R) (2012).

[50] H. Shi, H. Pan, Y.-W. Zhang, and B. I. Yakobson, Phys. Rev. B **87**, 155304 (2013).

[51] T. C. Berkelbach, M. S. Hybertsen, and D. R. Reichman, Phys. Rev. B **88**, 045318 (2013).

[52] A. Ramirez-Torres, V. Turkowski, and T. S. Rahman, Phys. Rev. B **90**, 085419 (2014).

[53] T. C. Berkelbach, M. S. Hybertsen, and D. R. Reichman, Phys. Rev. B **92**, 085413 (2015).

[54] M. M. Fogler, L. V. Butov, and K. S. Novoselov, Nat. Commun. **5**, 4555 (2014).

[55] F. Ceballos, M. Z. Bellus, H.-Y. Chiu, and H. Zhao, ACS Nano **8**, 12717 (2014).

[56] G. Wang, X. Marie, L. Bouet, M. Vidal, A. Balocchi, T. Amand, D. Lagarde, and B. Urbaszek, Appl. Phys. Lett. **105**, 182105 (2014).

[57] F.-C. Wu, F. Xue, and A. H. MacDonald, Phys. Rev. B **92**, 165121 (2015)

[58] D. S. Jin, M. R. Matthews, J. R. Ensher, C. E. Wieman, and E. A. Cornell, Phys. Rev. Lett. **78**, 764 (1997).

[59] P. Öhberg and S. Stenholm, Phys. Rev. A **57**, 1272 (1998).

[60] E. Altman, W. Hofstetter, E. Demler, and M. D. Lukin, New J. Phys. **5**, 113 (2003).

[61] K. Kasamatsu, M. Tsubota, and M. Ueda, Phys. Rev. Lett. **91**, 150406 (2003).

[62] P. Tommasini, E. J. V. de Passos, A. F. R. de Toledo Piza, M. S. Hussein, and E. Timmermans, Phys. Rev. A **67**, 023606 (2003).

[63] C.-Y. Lin, E. J. V. de Passos, A. F. R. de Toledo Piza, D.-S. Lee, and M. S. Hussein, Phys. Rev. A **73**, 013615 (2006).

[64] B. Sun and M. S. Pindzola, J. Phys. B: At., Mol. Opt. Phys. **43**, 055301 (2010).

[65] A. A. Abrikosov, L. P. Gorkov, and I. E. Dzyaloshinskii, *Methods of Quantum Field Theory in Statistical Physics* (Prentice-Hall, Englewood Cliffs, NJ, 1963).

[66] E. M. Lifshitz and L. P. Pitaevskii, *Statistical Physics*, Part 2 (Pergamon, Oxford, 1980).

[67] O. L. Berman, R. Ya. Kezerashvili, and K. Ziegler, Phys. Rev. A **87**, 042513 (2013).

[68] J. Sabio, F. Sols, and F. Guinea, Phys. Rev. B **81**, 045428 (2010).

[69] D. Y. Qiu, F. H. da Jornada, and S. G. Louie, Phys. Rev. Lett. **111**, 216805 (2013).

[70] P. Cudazzo, I. V. Tokatly, and A. Rubio, Phys. Rev. B **84**, 085406 (2011).

[71] E. V. Calman, C. J. Dorow, M. M. Fogler, L. V. Butov, S. Hu, A. Mishchenko, and A. K. Geim, Appl. Phys. Lett. **108**, 101901 (2016).

[72] L. V. Keldysh, Zh. Eksp. Teor. Fiz. Pis. Red. **29**, 716 (1979) [JETP Lett. **29**, 658 (1979)].

[73] Y. You, X.-X. Zhang, T. C. Berkelbach, M. S. Hybertsen, D. R. Reichman, and T. F. Heinz, Nat. Phys. **11**, 477 (2015).

[74] O. L. Berman, Yu. E. Lozovik, and G. Gumbs, Phys. Rev. B **77**, 155433 (2008).

[75] B. Laikhtman, J. Phys.: Condens. Matter **19**, 295214 (2007).

[76] O. L. Berman, R. Ya. Kezerashvili, and Yu. E. Lozovik, Phys. Rev. B **78**, 035135 (2008).

[77] O. L. Berman, R. Ya. Kezerashvili, and Yu. E. Lozovik, Phys. Lett. A **372**, 6536 (2008).

[78] C. Ciuti, V. Savona, C. Piermarocchi, A. Quattropani, and P. Schwendimann, Phys. Rev. B **58**, 7926 (1998).

[79] S. B.-T. de-Leon and B. Laikhtman, Phys. Rev. B **63**, 125306 (2001).

[80] C. Ciuti, P. Schwendimann, and A. Quattropani, Semicond. Sci. Technol. **18**, S279 (2003).

[81] O. L. Berman, R. Ya. Kezerashvili, and K. Ziegler, Phys. Rev. B **86**, 235404 (2012).

[82] X. Liu, T. Galfsky, Z. Sun, F. Xia, E.-C. Lin, Y.-H. Lee, Stéphane Kéna-Cohen, and V. M. Menon, Nat. Photon. **9**, 30 (2015).

[83] A. Chernikov, A. M. van der Zande, H. M. Hill, A. F. Rigosi, A. Velauthapillai, J. Hone, and T. F. Heinz, Phys. Rev. Lett. **115**, 126802 (2015).